

Study of the Structural, Elastic, Electronic and Optical Properties of the Ternary Acetylides A_2MC_2 ($A = Na, K$) and ($M = Pb, Pt$)

M. A. GHEBOULI

*Department of Chemistry, Faculty of Technology,
University of Mohamed Boudiaf, M'sila, 28000, Algeria and
Research Unit on Emerging Materials (RUEM), University of Ferhat Abbas, Setif 01, 19000, Algeria*

B. GHEBOULI

*Laboratory of Surface and Interface Studies of Solid Materials,
Department of Physics, Faculty of Science, Setif University 1, 19000, Algeria*

M. FATMI* and T. CHIH

Research Unit on Emerging Materials (RUEM), University of Ferhat Abbas, Setif 01, 19000, Algeria

(Received 11 December 2017, in final form 3 September 2018)

We studied the ternary acetylides A_2MC_2 ($A = Na, K$) and ($M = Pb, Pt$) with trigonal structures by using the density functional theory (DFT) as implemented in the CASTEP code. The calculated lattice parameters and atomic fractional coordinates were in agreement with previous calculations and experimental data. A set of isotropic elastic parameters and related properties, namely the module and shear moduli, Young's modulus, Poisson's ratio, average sound velocity and Debye temperature were numerically estimated in the frame work of the Voigt-Reuss-Hill approximation. The absorption, energy-loss and dielectric function were calculated. We studied the main contribution to the optical spectra from the transition from the top four valence bands towards the lower three first one of conduction based on the electronic structures.

PACS numbers: 31.15.ae, 42.25.-p, 62.20.de, 63.20.dk, 62.20.dj

Keywords: Ternary acetylides, Trigonal structure, Electronic structures

DOI: 10.3938/jkps.75.678

I. INTRODUCTION

The ternary acetylides with the composition A_2MC_2 where $A = Na$ or K and $C = Pd$ (4d) or Pt (5d) are interesting semiconducting materials. These materials can be synthesized by using solid state reaction of A_2C_2 with palladium or platinum in an inert atmosphere at a temperature of about $350^\circ C$ [1–5]. A_2C_2 was synthesized by reacting elemental sodium (potassium) with acetylene gas in $lq-NH_3$, by heating the resulting $NaC_2H(KC_2H)$ at $155^\circ C$ under vacuum as described in Ref. 6. Measurements of the electrical conductivity and band structure indicate that these compounds are semiconductors [7]. These types of materials are used in electron guns for synchrotrons, electron lasers and night vision devices. The studied ternary acetylides have a trigonal structure with space group ($P3m1, 164$). The structural characterization indicates that these compounds have the lattice parameters a and c and the atomic fractional coordi-

nates z_A and z_C . The atomic positions in the unit cell are $M: 1a (0,0,0)$, $A: 1d(1/3,1/3,z_A)$, and $C: 2c (0, 0, z_C)$. Recently, Suetin and Ivanovskii performed a theoretical study of the structural parameters at equilibrium and the electronic properties of these compounds by using the full-potential method within the mixed basis APW+ plp (FLAPW) implemented in the Wien2k [8]. The goal of the present work was to perform a detailed theoretical investigation of the structural, elastic, electronic and optical properties of the A_2MC_2 ($A = Na, K$) and ($M = Pb, Pt$) family by using the density functional theory (DFT) as implemented in the CASTEP code. The models and methodology will be given in Sec. II. The calculated results and discussion will be presented in Sec. III. The conclusion of the present investigation will be given in Sec. IV.

*E-mail: fatmimessaoud@yahoo.fr

II. MODELS AND METHODOLOGY

All calculations performed using a first-principles plane-wave pseudo-potential method based on DFT implemented in the CASTEP code [9]. The interactions of valence electrons with ion cores represented by Vanderbilt-type ultrasoft pseudopotentials [10] for Na, K, Pd, Pt and C atoms. The generalized gradient approximation of Perdew, Burke and Ernzerhof [11] was adopted for the exchange-correction functional. The special points sampling integration over the Brillouin zone was employed by using the Monkhorst-Pack method [12] with $8 \times 8 \times 8$ k -point meshes. The cut-off energy was set as 360 eV. We optimized the lattice parameters a and the atomic fractional coordinates z_A and z_C at a fixed volume of the unit cell which corresponds to the minimum energy. We observe the same number of valence bands in these compounds. The valence electrons are transferred from the Pt-d or Pd-d or C-p orbital to the Na-p or K-P site. The strong hybridization between Pt-d or Pd-d orbitals and C-p states in the upper valence banding region indicates the existence of a covalent bonding character. The overall shapes of the DOS and partial DOS (PDOS) are quit similar in the investigated compounds, indicating their similar chemical bonding. The structural parameters were determined using the Broyden-Fletcher-Goldfarb-Shanno minimization technique [13].

III. RESULTS AND DISCUSSIONS

1. Crystal structure

The ternary acetylides A_2MC_2 ($A = \text{Na, K}$) and ($M = \text{Pb, Pt}$) compounds crystallized in a trigonal structure with space group ($P\bar{3}m1$, $\neq 164$). This series is characterized by lattice parameters a and C and by atomic fractional coordinates z_A and z_C . We report in Table 1 the results of optimized lattice parameters a and C and the internal coordinates z_A and z_C . Also, shown for comparison are their available experiment data for the lattice parameters (a, c) of Na_2PdC_2 (4.464 and 5.218 Å), K_2PdC_2 (5.105 and 5.282 Å) and K_2PtC_2 (5.123 and 5.218 Å) quoted in Ref. 7, which agree well with our results. Our atomic fractional coordinate z_A for K_2PdC_2 and K_2PtC_2 are closer to the experiment values 0.278 and 0.275 [7]. Our results for the lattice parameters a and c and the atomic fractional coordinates z_A and z_C concerning the compound Na_2PtC_2 are predictions.

Under hydrostatic pressure in the range 0–20 GPa, the normalized volume shown in Fig. 1 decreases monotonously by following hyperbolic form. The bulk modulus and its pressure derivative for the ternary acetylides compounds determined from the P-V data for the Birch Equation Of State (EOS) [14]. are reported in Table 1. No experimental or theoretical results for the

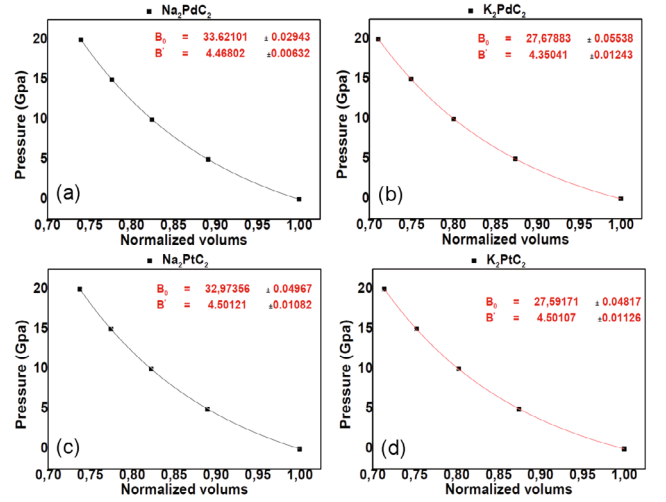


Fig. 1. (Color online) Normalized volume as a function of pressure for the (a) Na_2PdC_2 , (b) K_2PdC_2 , (c) Na_2PtC_2 , and (d) K_2PtC_2 compounds.

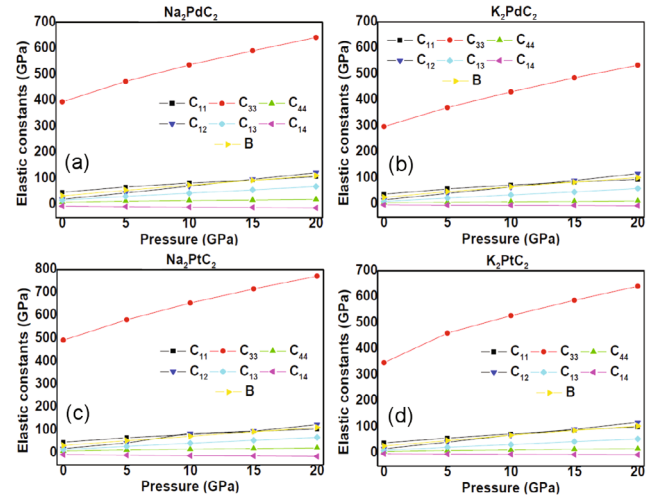


Fig. 2. (Color online) Effect of pressure on the elastic constants of the (a) Na_2PdC_2 , (b) K_2PdC_2 , (c) Na_2PtC_2 , and (d) K_2PtC_2 compounds.

bulk modulus and its pressure derivative for these compounds, So our computed values are predictions. We noticed that the DFT underestimates the studied lattice parameters, atomic fractional coordinates and bulk modulus.

2. Elastic constants

The elastic constants were determined by using a perturbation method. The elastic moduli at equilibrium pressure predicted by GGA functional for A_2MC_2 ($A = \text{Na, K}$) and ($M = \text{Pb, Pt}$) are listed in Table 1. The bulk modulus calculated from the elastic constants has nearly the same value as that obtained from the equation of state (EOS). This may be an estimate of the re-

Table 1. Optimized lattice parameters (a and c , in Å), internal coordinates (z_S , z_{Sr}), bulk modulus (B_0 , in GPa), and bulk modulus pressure derivative (B').

	Na ₂ PdC ₂		K ₂ PdC ₂		Na ₂ PtC ₂		K ₂ PtC ₂	
	This work	Exp.	This work	Exp.	This work	Exp.	This work	Exp.
Lattice constant a (Å)	4.4383	4.464 ¹	5.0188	5.105 ¹	4.4919		5.055	5.123 ¹
Lattice constant c (Å)	5.2555	5.266 ¹	5.2714	5.282 ¹	5.2276		5.244	5.218 ¹
Z_A atom position	0.2789		0.2762	0.278 ¹	0.2686		0.269	0.275 ¹
Z_C atom position	0.3791		0.3792		0.3780		0.3784	
B (GPa)	33.62		27.671		32.971		27.67	
B'	4.47		4.35		4.5		4.35	
C_{11} (GPa)	47.57		38.12		48.27		38.78	
C_{33} (GPa)	394.7		297.68		492.44		347.07	
C_{44} (GPa)	9.35		5.51		9.84		5.26	
C_{12} (GPa)	20.54		16.22		20.21		16.25	
C_{13} (GPa)	16.61		10.47		16.17		9.33	
C_{14} (GPa)	-6.09		-3.07		-6.3		-3.31	
B^* (GPa)	33.29		26.25		33.58		26.65	
B'^*	4.26		4.29		4.14		4.3	
G	27.44		19.9		28.93		21.48	
E	68.1		49.77		71.15		53.69	
σ	0.24		0.25		0.23		0.25	
ρ	1.59		1.67		1.51		1.66	
B/G	1.22		1.31		1.16		1.24	
v_l (m·s ⁻¹)	6418		5750		5366		5023	
v_t (m·s ⁻¹)	4566		4064		3843		3553	
v_m (m·s ⁻¹)	4946		4407		4158		3852	
θ_D	495		429		474		421	
[100]								
V_L (m·s ⁻¹)	3816		3557		2615		3019	
V_{T1} (m·s ⁻¹)	2507		2320		2048		1954	
V_{T2} (m·s ⁻¹)	1692		1352		1429		1112	
[001]								
V_L (m·s ⁻¹)	10993		9940		10109		9033	
V_{T1} (m·s ⁻¹)	1692		1352		1429		1112	
V_{T2} (m·s ⁻¹)	1692		1352		1429		1112	

liability and accuracy of our computed elastic constants. Our results related to equilibrium and under pressure are predictions. One condition for the mechanical stability of a structure is that its strain energy must be positive against any homogeneous elastic deformation. For a trigonal crystal, the mechanical stability under isotropic pressure is judged based on the following condition [15]:

$$\begin{aligned} C_{11} > C_{12}, \quad C_{33}(C_{11} + C_{12}) > 2C_{13}^2, \\ C_{44}(C_{11} + C_{12}) > 2C_{14}^2. \end{aligned} \quad (1)$$

Our calculated elastic constants for this series of ternary acetylides compounds satisfy all these above criteria over the pressure range 0–20 GPa, indicating their mechanical stability. The effect of the pressure on the elastic moduli is visualized in Fig. 2. We noticed that these compounds

show low elastic constants. Their variation is little sensitive to the pressure. The lower values of the elastic constants indicate that the studied compounds have a weak hardness. The elastic constant C_{11} in all three compounds is smaller than C_{33} , indicating the presence of a big resistance due to the compression along the (001) direction and the caxis is less compressible than the a axis.

The crystals are usually synthesized in the polycrystalline form. The bulk and the shear moduli B and G are two important mechanical quantities for technological and engineering applications. The bulk modulus represents the resistance to fracture, while the shear modulus, which represents the resistance to plastic deformation, is related to bond bending and depends on the nature of the bond. We estimated the elastic characteristics

of polycrystalline materials by using the Voigt-Reuss-Hill (VRH) procedure [16–18]. Hill proved that the Voigt and Reuss equations represent upper and lower limits on the true polycrystalline constants. He showed that the polycrystalline moduli B and G are the arithmetic mean values in the Voigt and Reuss approximations. The VRH approximation is the average of the lower bound of Voigt and the upper bound of Reuss, which for a method to estimating the mechanical properties of crystalline materials with elastic constants for single crystals [19]. We reported in Table 1 the bulk modulus B , shear modulus G , Young's modulus Y and Poisson's ratio σ obtained by using the following relations with the VRH approximation [19]:

$$B = \frac{1}{2}(B_R + B_V), \quad (2)$$

$$G = \frac{1}{2}(G_R + G_V), \quad (3)$$

$$Y = \frac{9BG}{3B + G}, \quad (4)$$

$$\sigma = \frac{3B - Y}{6B}, \quad (5)$$

where

$$B_R = \frac{C_{33}(C_{11} + C_{12}) - 2C_{13}^2}{C_{11} + C_{12} + 2C_{33} - 4C_{13}}, \quad (6)$$

$$B_V = \frac{1}{9}[2(C_{11} + C_{12}) + C_{33} + 4C_{13}], \quad (7)$$

$$G_V = \frac{1}{30}[C_{11} + C_{12} + 2C_{33} - 4C_{13} + 12C_{44} + 12C_{66}], \quad (8)$$

$$G_R = \frac{5}{2} \frac{[C_{33}(C_{11} + C_{12}) - 2C_{13}^2]^2 C_{33}(C_{11} + C_{12}) - 2C_{13}^2}{3B_V C_{44} C_{66} + (C_{44} + C_{66})[C_{33}(C_{11} + C_{12}) - 2C_{13}^2]^2}$$

with $C_{66} = \frac{1}{2}(C_{11} - C_{12})$. (9)

We note that the lower values of the bulk modulus and the shear modulus correspond to a weaker resistance to volume change caused by pressure and directional bonding between atoms.

We found that Y is weaker for all series, indicating their lower stiffness. The estimated Poisson's ratio are lower than the limit value (0.25) [20], suggesting that these compounds have lower lateral expansion, are affected by size of no central forces and reveal the presence of a covalent bonding character. The ratio of the shear modulus to the bulk modulus B/G of crystalline material are proposed by Pugh [21] can be considered as an indication of the extent of fracture in these materials. The calculated B/G values are smaller than the critical value (0.75), classifying these materials as brittle. Then, all these compounds can support large thermal shocks.

The Debye temperature may be estimated from the average sound velocity ν_M [22].

$$\theta = \frac{h}{k} \left[\frac{3n}{4\pi} \left(\frac{N_A \rho}{M} \right) \right]^{1/3} \nu_m, \quad (10)$$

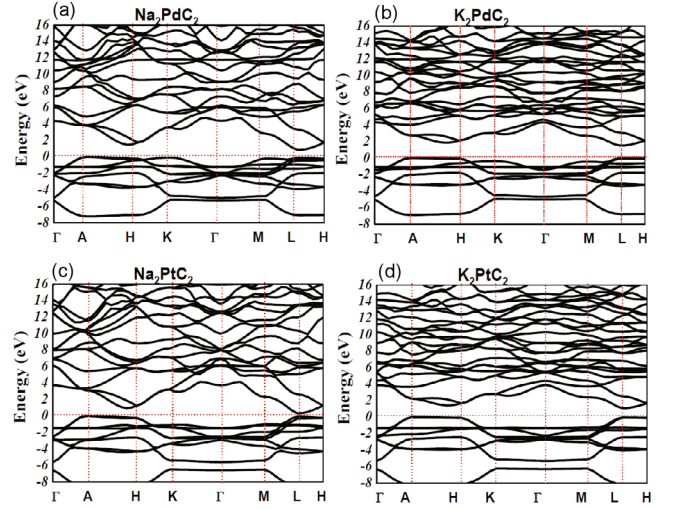


Fig. 3. (Color online) Band structures of the (a) Na_2PdC_2 , (b) K_2PdC_2 , (c) Na_2PtC_2 , and (d) K_2PtC_2 compounds.

where h , k , N_A , n , M , ρ and ν_m are respectively Planck's constant, Boltzmann's constant, Avogadro's number, the number of atoms per formula unit, the molecular mass per formula unit, the density and the average sound velocity obtained from the relation [22]:

$$\nu_m = \left[\frac{1}{3} \left(\frac{2}{\nu_s^3} + \frac{1}{\nu_l^3} \right) \right]^{-1/3}, \quad (11)$$

where ν_s and ν_l are, respectively, the shear and the longitudinal sound velocities obtained from Navier's equation [23]:

$$\nu_t = \sqrt{\frac{G}{\rho}} \quad \text{and} \quad \nu_l = \sqrt{\frac{B + \frac{4}{3}G}{\rho}}. \quad (12)$$

The calculated elastic wave velocities along the [100], [110] and [111] directions, the density ρ , the sound velocities ν_l , ν_t and ν_m and the Debye temperature θ_D are reported in Table 1. The longitudinal waves are fastest along the [001] direction and the shear waves are slowest along the [001] direction for these compounds. The results for the density ρ , the sound velocities ν_l , ν_t , and ν_m and the Debye temperature θ_D reported in Table 1. because no data for their parameters are available in the literature, then our results are considered to be predictions.

3. Electronic properties

The energy band structures of A_2MC_2 ($\text{A} = \text{Na}, \text{K}$) and ($\text{M} = \text{Pb}, \text{Pt}$) along the higher symmetry directions in the Brillouin zone at the equilibrium geometry calculated by the GGA calculation are plotted in Fig. 3. K_2PtC_2 and K_2PdC_2 show $A - A$ direct gaps of 1.09 and 1.57 eV respectively. While Na_2PdC_2 and Na_2PtC_2

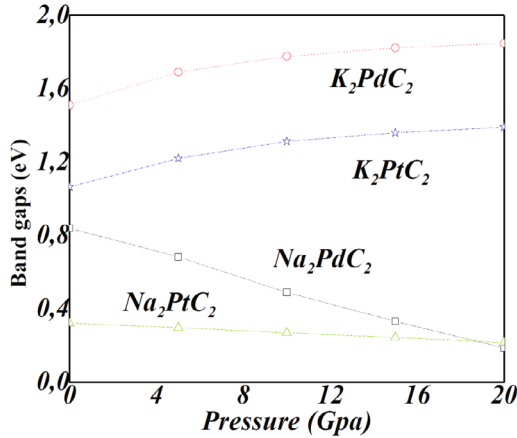


Fig. 4. (Color online) Pressure dependence of the band gaps of the Na_2PdC_2 , K_2PdC_2 , Na_2PtC_2 , and K_2PtC_2 compounds.

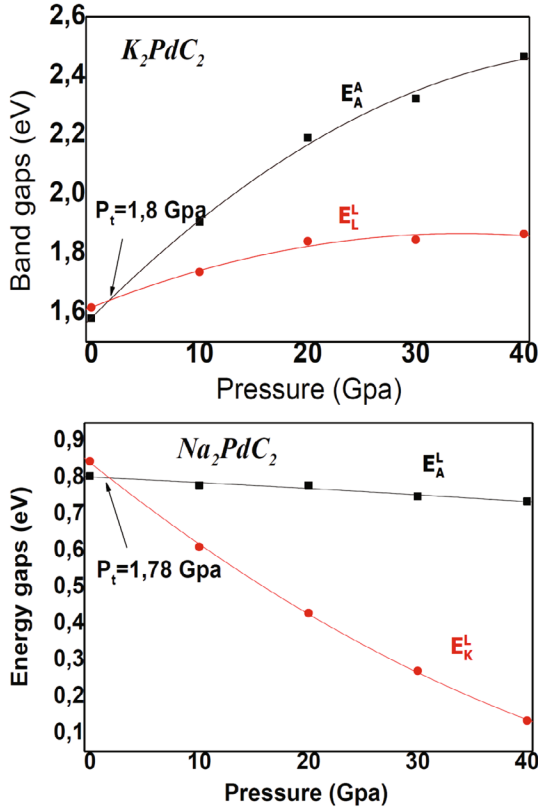


Fig. 5. (Color online) Pressure dependence of the transition gaps of the K_2PdC_2 , Na_2PtC_2 compounds.

present A-L indirect gaps of 0.84 eV and 0.31 eV. No experimental data for the band gap are available in the literature, so our results are predictions. We display in Fig. 4 the dependence on pressure of the direct and indirect band gaps for these compounds. The fundamental gaps of Na_2PdC_2 and Na_2PtC_2 decrease monotonically with increasing pressure, while for K_2PtC_2 and K_2PdC_2 , increase. In Fig. 5, under a pressure, we notice transi-

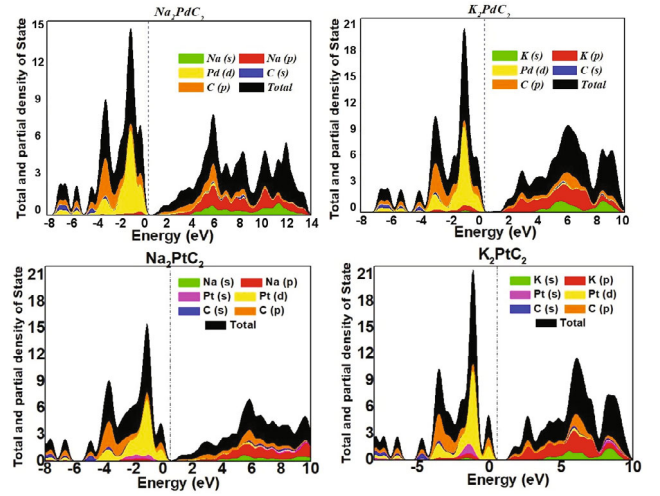


Fig. 6. (Color online) Partial and total densities of states of the K_2PdC_2 and the Na_2PdC_2 .

tions from A – A to L – L gap in K_2PdC_2 and K_2PtC_2 , there occurs at 1.8 and 13 GPa respectively. While, for Na_2PdC_2 a transition from A-L to K-L gap which occurs at 1.78 GPa. No transition gap is observed in the Na_2PtC_2 compound. The fundamental gap as a function of pressure can be expressed by :

$$\begin{aligned} E_g^{\text{Na}_2\text{PdC}_2} &= 0.84 - 0.03P + 1.7 \times 10^{-4}P^2, \\ E_g^{\text{K}_2\text{PdC}_2} &= 1.57 + 0.03P - 0.01P^2, \\ E_g^{\text{Na}_2\text{PtC}_2} : E_g &= 0.31 - 0.005P - 1.14 \times 10^{-5}P^2, \\ E_g^{\text{K}_2\text{PtC}_2} &= 1.09 + 0.03P - 8.48 \times 10^{-4}P^2. \end{aligned} \quad (13)$$

The partial density of states (PDOS) of A_2MC_2 ($\text{A} = \text{Na}, \text{K}$) and ($\text{M} = \text{Pd}, \text{Pt}$) as shown in Fig. 6 reveal that the upper valence bands consisted of Pt-d and C-p orbitals. The upper valence band is located between at $-2.79, -2.43, -2.23$, and 1.88 eV and the Fermi level for Na_2PtC_2 , K_2PtC_2 , Na_2PdC_2 and K_2PdC_2 respectively. We observe the same number of valence bands in these compounds. The valence electrons are transferred from the Pt-d or Pd-d or C-p orbital to the Na-p or K-p site. The strong hybridization between the Pt-d or Pd-d orbital and C-p states in the upper valence bonding region translates the existence of a covalent bonding character. The overall shapes of the DOS and the partial DOS are quite similar in the investigated compounds, indicating their similar chemical bonding.

4. Optical properties

We show in the Fig. 7 the real and the imaginary parts of the dielectric functions of Na_2PdC_2 and K_2PdC_2 as functions of the photons energy. The imaginary part of the dielectric function is directly connected with the

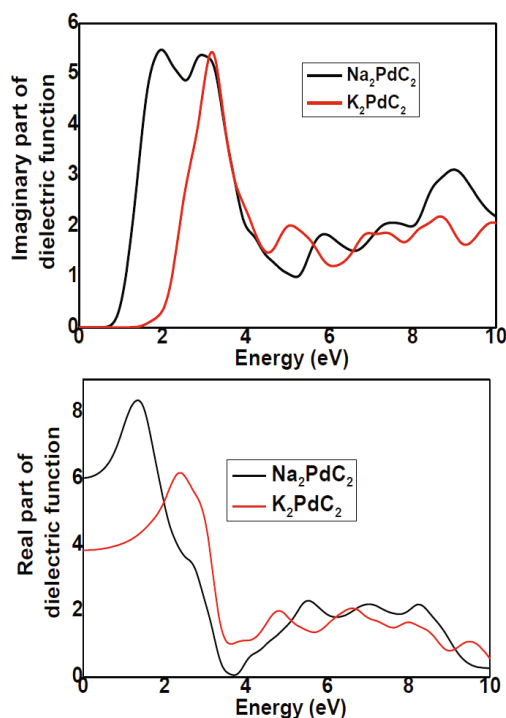


Fig. 7. (Color online) (a) Imaginary and (b) real parts of the dielectric function of the A_2MC_2 ($A = Na, K$) and ($M = Pb, Pt$) compounds as function of the energy.

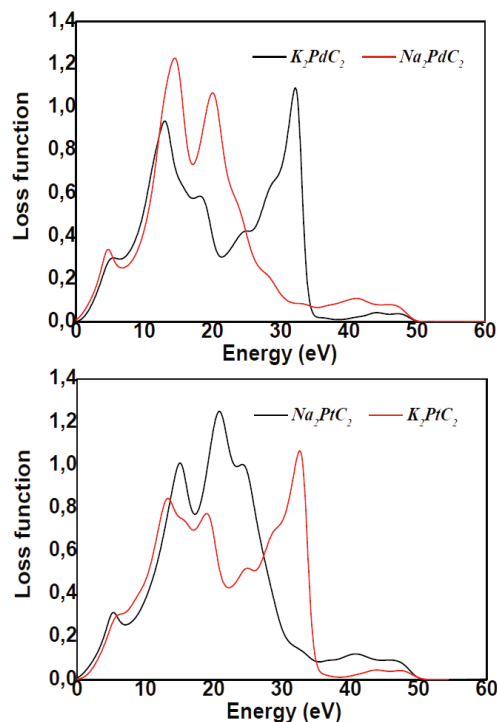


Fig. 9. (Color online) Loss function as function of photon energy of the the A_2MC_2 ($A = Na, K$) and ($M = Pb, Pt$) compounds.

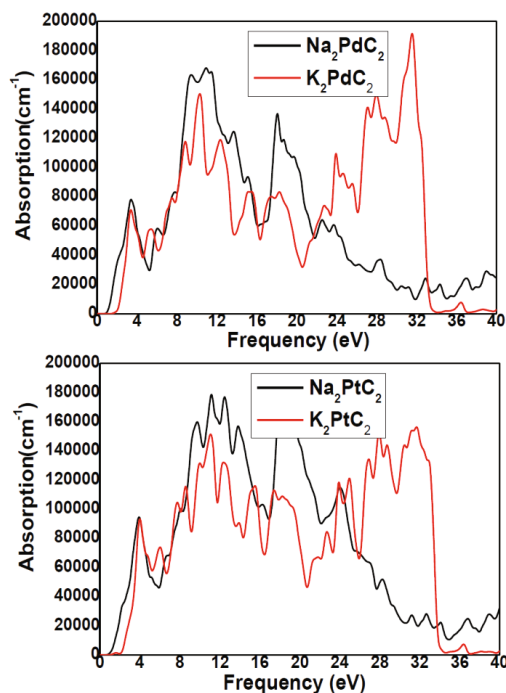


Fig. 8. (Color online) Absorption as a function of photon frequency of the the A_2MC_2 ($A = Na, K$) and ($M = Pb, Pt$) compounds.

energy band structure. The static optical dielectric constants of Na_2PdC_2 and K_2PdC_2 are respectively 3.76

and 6.08, and increase with energy in the transparency region, reaching peaks in the ultraviolet at about 2.38 eV and 1.34 eV. The minima of the static dielectric constant, 0.99 and 0.1 occur at an energy of 3.62 eV for Na_2PdC_2 and K_2PdC_2 . The optical absorption started at 1.27 eV, 0.66 eV, 1.06 eV and 0.9 eV in K_2PdC_2 , Na_2PdC_2 , K_2PtC_2 and Na_2PtC_2 , respectively, as shown in Fig. 8. The maximum absorption occurs at about 11 eV. The electron energy loss function, which is an important factor describing the energy loss of a fast electron traversing a material, is also shown in Fig. 9. The peaks in this spectrum represent the characteristics associated with the plasma resonance and the corresponding frequency is the so-called plasma frequency w_p . The energy-loss peaks correspond to the trailing edges in the reflection spectra; for instance, the prominent loss peaks are situated at energies corresponding to abrupt reductions of reflectivity. We note that the relative spectra of K_2PdC_2 (Na_2PdC_2) are identical to those of K_2PtC_2 (Na_2PtC_2). A maximum loss of 109% (127%) is obtained for an energy of 32.18 eV (20 eV) for Na_2PdC_2 (K_2PtC_2) and Na_2PtC_2 (K_2PtC_2).

In order to determine the origins of the different peaks and features of K_2PtC_2 , we plotted the transition energy $E(k) = E_{C_j}(k) - E_{V_i}(k)$ in Fig. 10; V_i is the valence band number i and C_j is the conduction band number j . The main contribution to the optical spectra originates from the transition from the top four valence bands to the lower three conduction bands. The edge of

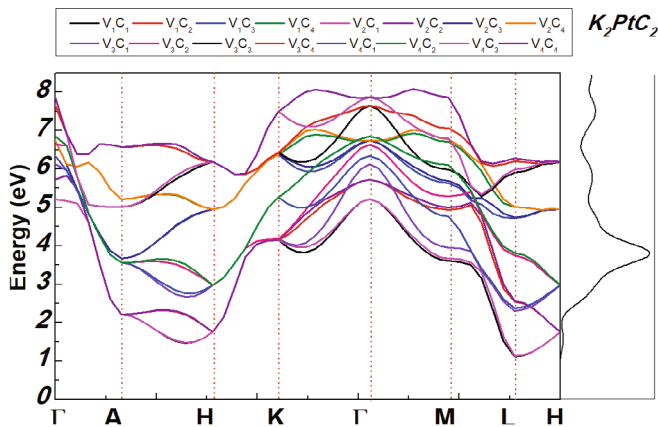


Fig. 10. (Color online) The transition energy $E(k) = E_{C_j}(k) - E_{V_i}(k)$ of the A_2MC_2 ($A = Na, K$) and ($M = Pb, Pt$) compounds.

the optical absorption located at 1.06 eV in K_2PtC_2 is probably caused by transition bands $V_1 - C_1$ or $V_4 - C_3$ at L point in the Brillouin zone which corresponds to the direct gap $A - A$. The first peak positioned at 1.5 eV is due probably to the transition band $V_1 - C_1$ in L point. The structure centered at 3.79 eV originates mainly from transition bands $V_3 - C_2$ and $V_4 - C_2$ at the L point. The peak located at 5.7 eV comes from transition bands $V_1 - C_2$ and $V_2 - C_2$ at the Γ point. The transition bands $V_4 - C_4$ and $V_4 - C_3$ at the K point and $V_3 - C_4$ and $V_3 - C_3$ at the Γ point correspond to the energy 7.5 eV.

IV. CONCLUSION

Employing a pseudo-potential plane-wave approach based on the density functional theory, within the generalized gradient approximation, we investigated the structural, elastic, electronic and optical properties of the ternary acetylides A_2MC_2 ($A = Na, K$) and ($M = Pb, Pt$). We predicted the average sound velocity, the Debye temperature and the elastic wave velocities of all these compounds. The calculated band structures show that K_2PtC_2 and K_2PdC_2 (Na_2PdC_2 and Na_2PtC_2) are $A - A$ direct ($A - L$ indirect) gap semiconductors. The ternary acetylides A_2MC_2 ($A = Na, K$) and ($M = Pb,$

Pt) are mechanically stable, show weak hardness, have lower stiffness and lateral expansion, and are classified as brittle materials. The PDOS indicates that the valence electrons are transferred from the Pt-d, Pd-d or C-p orbital to the Na-p or K-p site. The strong hybridization between Pt-d, Pd-d or C-p states in the upper valence bonding region indicates the existence of a covalent bonding character. We present various optical transitions between the top of the valence band and the bottom of the conduction band.

REFERENCES

- [1] M. H. Moissan, C. R. Acad. Sci. **126**, 302 (1898).
- [2] M. H. Moissan, C. R. Acad. Sci. **127**, 911 (1898).
- [3] H. Föppl, Angew. Chem. **70**, 401 (1958).
- [4] S. Hemmersbach, B. Zibrowius and U. Ruschewitz, Z. Anorg. Allg. Chem. **625**, 1440 (1999).
- [5] U. Ruschewitz, P. Müller and W. Kockelmann, Z. Anorg. Allg. Chem. **627**, 513 (2001).
- [6] K.-H. Klöss, D. Hinz-Hübner and U. Ruschewitz, Zeitschrift für anorganische und allgemeine Chemie **628**, 2701 (2002).
- [7] H. Billetter *et al.*, Z. Anorg. Allg. Chem. **636**, 1834 (2010).
- [8] D. V. Suetin and A. L. Ivanovskii, Mater. Sci. Semicond. Process. **19**, 72 (2014).
- [9] M. D. Segall *et al.*, J. Phys. Condens. Matter **14**, 2717 (2002).
- [10] D. Vanderbilt, Phys. Rev. B **41**, 7892 (1990).
- [11] J. P. Perdew, K. Burke and M. Ernzerhof, Phys. Rev. Lett. **77**, 3865 (1996).
- [12] H. J. Monkhorst and J. D. Pack, Phys. Rev. B **13**, 5188 (1976).
- [13] T. H. Fischer and J. Almlöf, J. Phys. Chem. **96**, 9768 (1992).
- [14] F. Birch, Phys. Rev. **71**, 809 (1947).
- [15] C. Jiang, Z. Lin and Y. Zhao, Scr. Mater. **63**, 532 (2010).
- [16] W. Voigt, *Lehrbuch der Kristallphysik* (Teubner, Leipzig, German, 1928), p. 716.
- [17] A. Reuss, Z. Angew. Math. Mech. **9**, 49 (1929).
- [18] R. Hill, Proc. Phys. Soc. London, Sect. A **65**, 349 (1952).
- [19] J. Feng *et al.*, Mater. Design **32**, 3231 (2011).
- [20] M. Mattesini *et al.*, Phys. Rev. B **79**, 125122 (2009).
- [21] S. F. Pugh, Philos. Mag. **45**, 823 (1954).
- [22] O. L. Anderson, J. Phys. Chem. Solids **24**, 909 (1963).
- [23] K. B. Panda and K. S. Ravi Chandran, Comput. Mater. Sci. **35**, 134 (2006).